Electronic Supplementary Information

Elie Geagea, Judicael Jeannoutot, Louise Morgenthaler, Simon Lamare, Alain Rochefort, Frank Palmino and Frédéric Chérioux

Univ. Bourgogne Franche-Comté, FEMTO-ST, UFC, CNRS, 15B avenue des Montboucons, 25030 Besançon Cedex
Polytechnique Montréal, Département de génie physique, Montréal, Canada H3C 3A7

1. Synthesis

All reagents were purchased from Aldrich, except $Pd(PPh_3)_4$ which was purchased from Strem chemical, and used as received. The silica gel used for column chromatography was purchased from Merck. The deuterated NMR solvents were purchased from Euriso-top. The NMR spectra were recorded using a Bruker AC-300 MHz spectrometer. 9,9'-bianthryl molecule was synthetized from the procedure of P. Natarajan *et al.*[1]

General procedure for the synthesis of 10,10'-di-(4''-cyanophenyl)-9,9'-bianthryl and 10,10'-di-(4''-pyridyl)-9,9'-bianthryl

This procedure is adapted from P. Natarajan *et al.*[1] and N. Miyaura *et al.*[2] 10,10'-dibromo-9,9'-bianthryl (200mg, 0.39 mmol) and 4'-cyanophenyl boronic acid pinacol ester (268mg, 1.17 mmol) or 4'-pyridyl boronic acid pinacol ester (268mg, 1.17 mmol) were dissolved in 70 mL of THF. Then, an aqueous solution of Cs_2CO_3 (0.5 M, 6 mL) and a $Pd(PPh_3)_4$ catalyst (45 mg, 0.04 mmol) were added. The resulting mixture was heated at 80°C overnight. Then, the solvent was removed under reduced pressure. The crude solid was dissolved in 40 mL of Chloroform and filtered over Celite. Then, the solvent was removed under reduced pressure. The resulting white solid was purified by column chromatography (silica gel, cyclohexane/dichloromethane 1:1) to give a white solid (90mg, 60%).

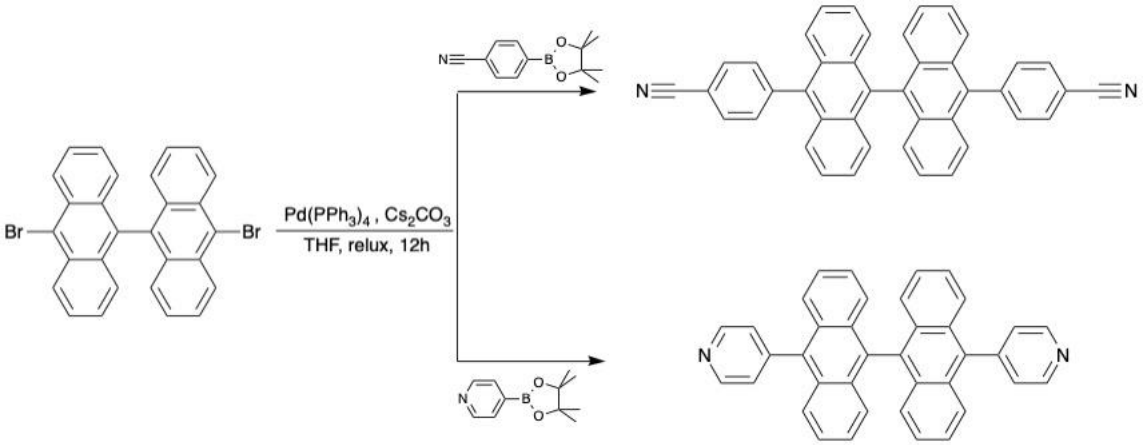

Scheme S1. Synthesis of 10,10'-di-(4''-cyanophenyl)-9,9'-bianthryl and 10,10'-di-(4''-pyridyl)-9,9'-bianthryl

10,10’-di-(4’’-cyanophenyl)-9,9’-bianthryl

^{1}H NMR (300 MHz, Chloroform-d) δ = 7.99 (d, J=8.35Hz, 4H), 7.78 (d, J=8.35 Hz, 4H), 7.68 (d, J=8.8 Hz, 4H), 7.36-7.40 (m, 4H), δ = 7.17-7.34 (m, 8H); ^{13}C NMR (75 MHz, Chloroform-d) δ = 144.38, 135.49, 134.17, 132.41, 131.21, 129.59, 127.15, 126.40, 126.02, 125.89, 118.89, 111.86.

a)

b)

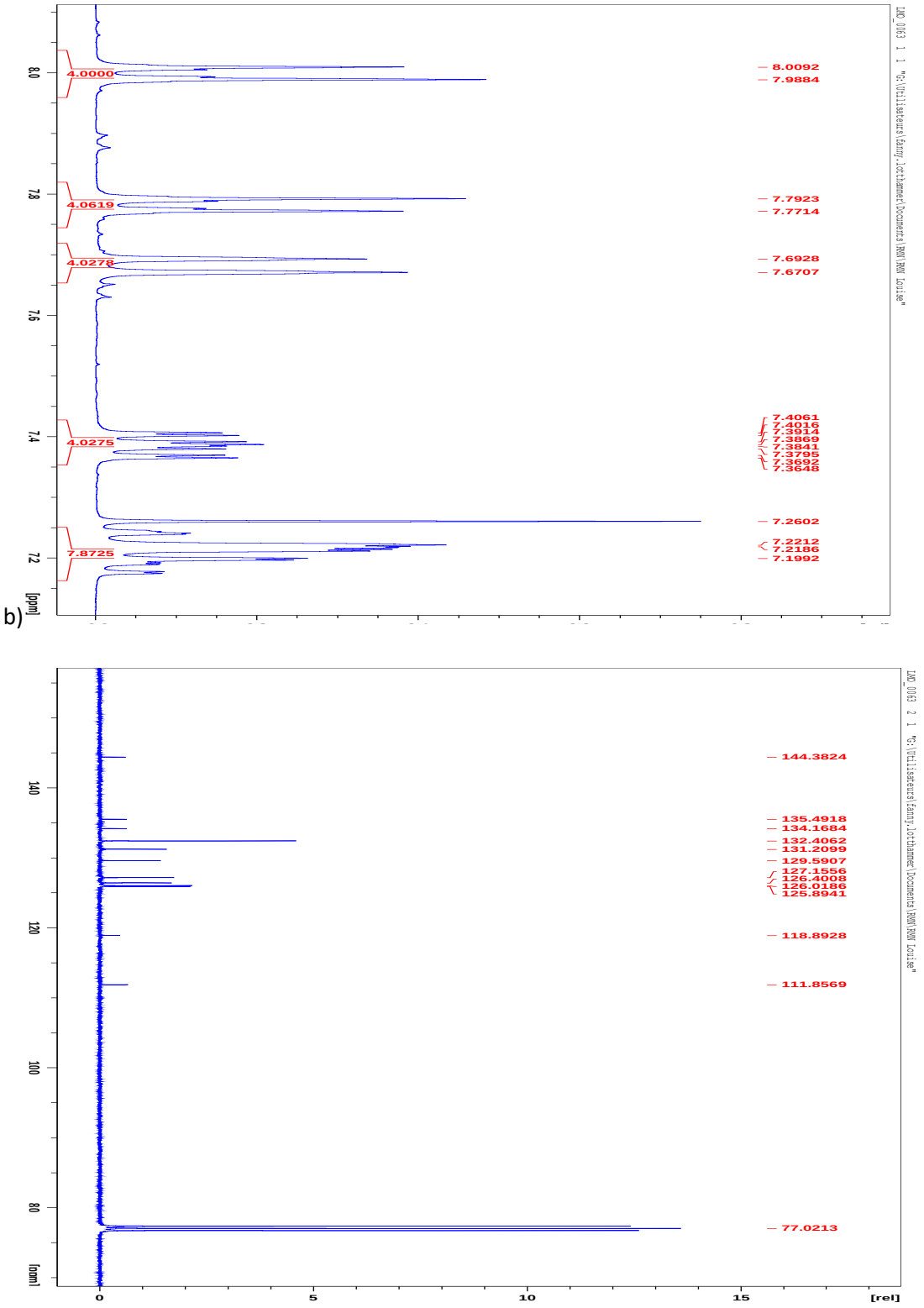

Fig. S1: a) ^{1}H and b) ^{13}C NMR spectra of 10,10’-di-(4’’-cyanophenyl)-9,9’-bianthryl

10,10’-di-(4’’-pyridyl)-9,9’-bianthryl

^{1}H NMR (300 MHz, Chloroform-d) δ = 8.96 (d, J=7.1 Hz, 4H), 7.73 (d, J=7.1 Hz, 4H), 7.62 (d, J=8.8 Hz, 4H), 7.39-7.43 (m, 4H), δ = 7.21-7.23 (m, 8H); ^{13}C NMR (75 MHz, Chloroform-d) δ = 148.11, 134.55, 133.72, 131.13, 129.13, 127.47, 127.19, 126.41, 126, 08, 126,02.

a)

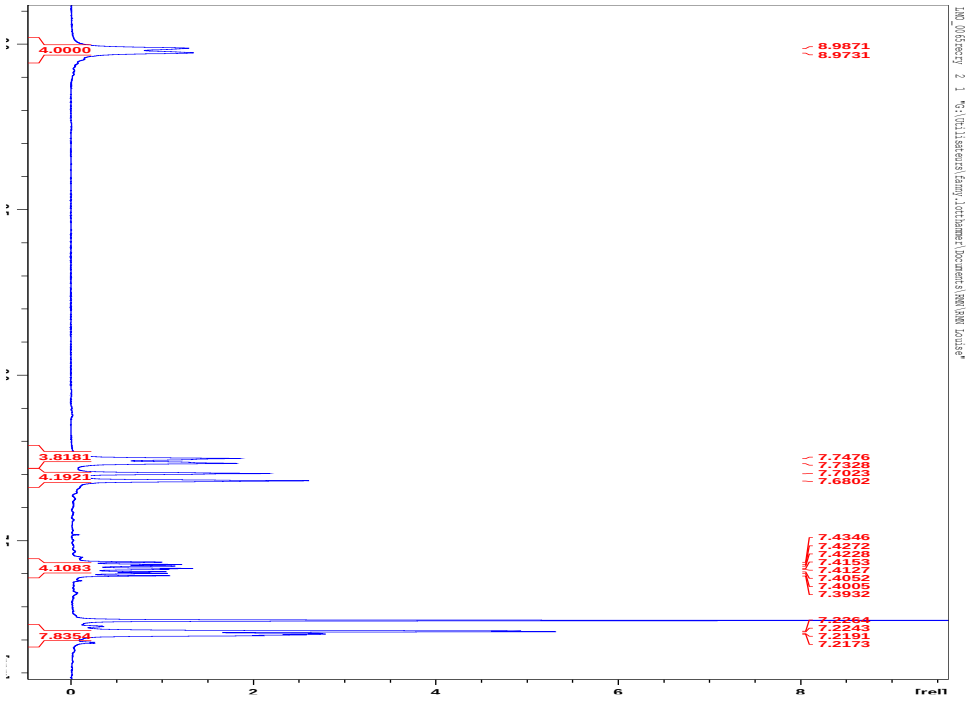

b)

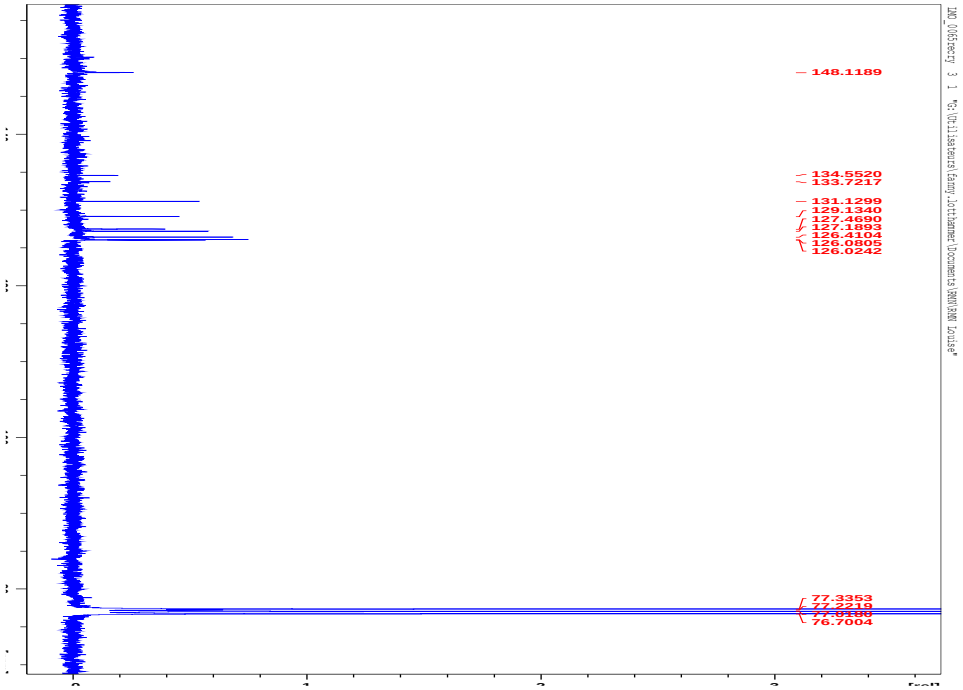

Fig. S2: a) ^{1}H and b) ^{13}C NMR spectra of 10,10’-di-(4’’-pyridyl)-9,9’-bianthryl

2. STM experiments

STM experiments were performed in an ultrahigh vacuum chamber with a base pressure lower than $2 \cdot 10^{-10}$ mbar equipped with a variable temperature Omicron Scanning Tunnelling Microscope. STM images were acquired in a constant current mode at 110 K. Metal substrate surfaces were cleaned with Argon ion sputtering at 1.2 kV followed by thermal annealing at 723K for Cu(111). All the molecules were deposited from a quartz crucible at corresponding temperature of sublimation for each: 418 K for BA, 458 K for PBA and 468 K for CPBA. The substrate was kept at room temperature during the sublimation. Each image process was carried out using SPIP software.

3. STM images

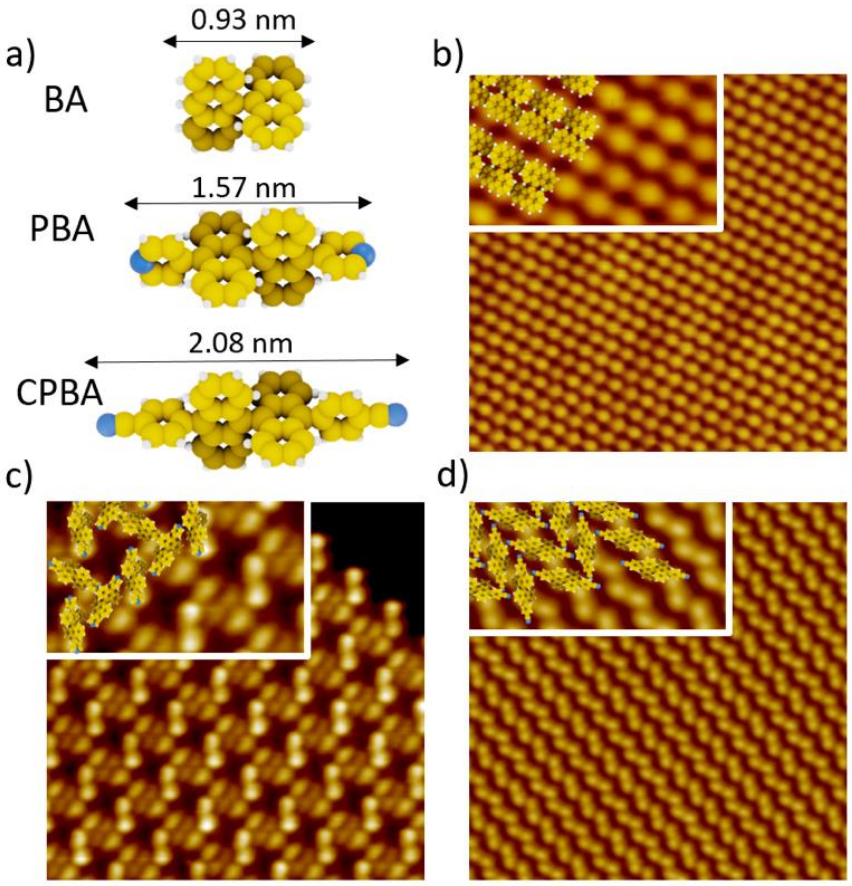

Fig. S3: a) CPK models of 9,9'-bianthryl (BA), 10,10'-di(4''-pyridyl)9,9'-bianthryl (PBA) and 10,10'-di(4''-cyanophenyl)9,9'-bianthryl (CPBA) molecules respectively. b) c) and d) STM images of supramolecular networks on Cu(111) surface of BA (V_s=1.8 V, I_t=1.01 nA, 15x15 nm²), PBA (V_s =0.9 V, I_t =10 pA, 15x15 nm²), and (V_s =-2.2 V, I_t =10 pA, 20x20 nm²) CPBA molecules, respectively.

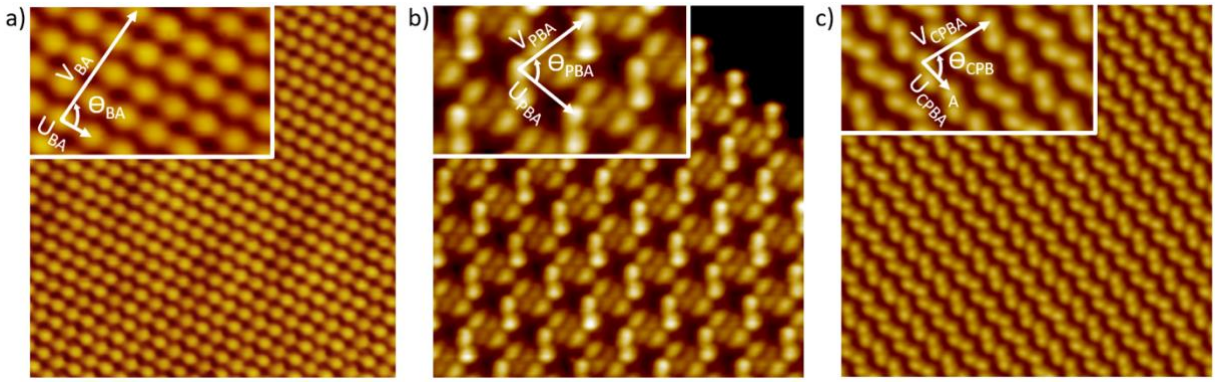

Fig. S4: STM images of supramolecular networks on Cu(111) surface with their corresponding unit cells. a) STM image of BA supramolecular networks on Cu(111) surface (Vs=1.8 V, It=1.01 nA, 15x15 nm²). The inset shows a zoomed area of the BA network (5x3 nm²) with corresponding unit cell vectors: **U_{BA} = 0.72 nm, U_{BA} = 2.67 nm, Θ_{BA} = 82°**. b) STM image of PBA supramolecular networks on Cu(111) surface (Vs =0.9 V, It =10 pA, 15x15 nm²). The inset shows a zoomed area of the PBA network (7x4 nm²) with corresponding unit cell vectors: **U_{PBA} = 1.98 nm, U_{PBA} = 2.20 nm, Θ_{PBA} = 77°**. c) STM image of CPBA supramolecular networks on Cu(111) surface (Vs =-2.2 V, It =10 pA, 20x20 nm²). The inset shows a zoomed area of the CPBA network (8x4 nm²) with corresponding unit cell vectors: **U_{CPBA} = 0.85 nm, U_{CPBA} = 1.63 nm, Θ_{CPBA} = 82°**.

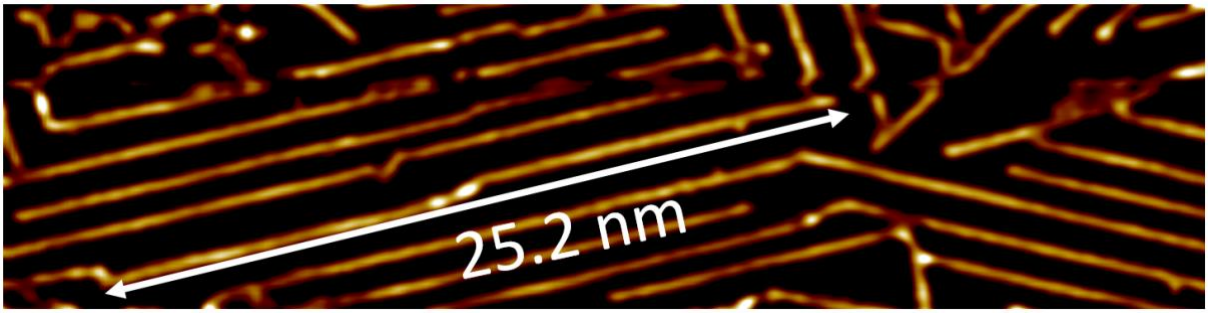

Fig. S5: STM image (V=-1.2 V, I=10 pA, 40x10 nm²) of the formed GNR after annealing of BA supramolecular network with the length of 25.2 nm

4. Density Functional Theory calculations

Density Functional Theory (DFT) calculations were carried out at T = 0 K with Siesta package[3] and the results were visualized with the Chimera software[4]. We used periodic boundary conditions with vdW-DF2 (or LMKLL) functional that includes van der Waals corrections. The computations were performed with norm-conserving Trouillier-Martins pseudopotentials and double-ζ polarized atomic basis sets. The mesh cut-off used to form the real space grid in the DFT calculations was 300 Ry, and the structural relaxation and geometry optimization were carried out using conjugate-gradient method until the forces and the variation of total energy were less than 0.01 eV/Å and 0.0001 eV, respectively. For the k-point sampling, a 12x12x1 mesh of the Monkhorst−Pack grid was used. We considered a vacuum region of 50 Å to minimize the interactions between periodic images in the direction normal to the slab. The

molecular species in the supercell were fully optimized while the Cu(111) surface slab containing four layers (144 atoms) was fixed to the bulk geometry.

We first consider the stability of gas phase or isolated molecular species, including the neutral and radical forms. In terms of electronic structure, Fig. S6 compares the projected density of states (PDOS) of hydrogen atoms in positions 2,2' to 10,10' for the BA adsorbed on Cu(111). The most important PDOS of C-H bonds closer to Fermi level are located at the 10,10' positions, hence they should be the more probably accessible with thermal excitation.

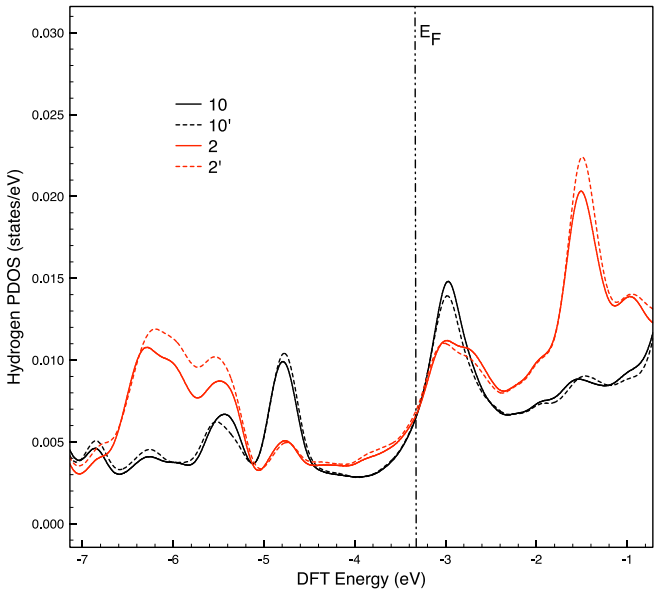

Fig. S6: Projected density of states (PDOS) of hydrogen atoms located at 10,10' and 2,2' positions for the adsorption of BA on Cu(111). Fermi level is indicated by the straight dashed line at -3.36 eV.

The following figure (Fig S7) shows the optimized geometry of the neutral BA molecule in gas phase where we have indicated the positions (2, 2', 10, 10') of the Hydrogen atoms involved in the reaction mechanism. The angle between the anthryl groups is around 90°. Removing H atoms at positions 2 and 2' or 10 and 10' does not introduce a significant variation of the geometry of the molecule. The 10,10' biradical is slightly more stable than the 2,2' specie by 40 meV.

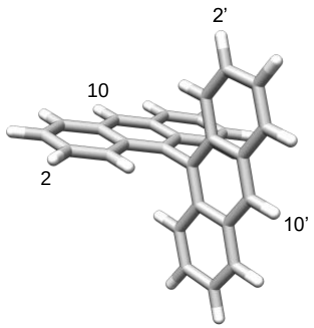

Fig. S7: DFT Simulation of BA molecule in vacuum.

The geometries of adsorbed species are shown below for neutral BA (a), 2,2'-bianthryl radical (b) and 10,10'-bianthryl radical (c) on the Cu(111) surface. The adsorption of neutral BA on Cu(111) is relatively stable, the calculated adsorption energy ($E_{BA}+E_{Cu(111)}-E_{BA/Cu(111)}$) is 3.32 eV/molecule. The geometry of adsorbed BA is quite different to the gas phase where the rings close to the Cu(111) surface become flatter that clearly indicate improved molecule-surface interactions.

Removing the H atoms in 2,2' or 10,10' positions introduce additional structural deformations of the molecular due to the formation of C-Cu bonds between radicals and surface Cu atoms (Fig S8). The DFT calculations indicate that 2,2'-BA/Cu(111) is more stable than 10,10'-BA/Cu(111) by around 290 meV. Our DFT results suggest that both adsorbed phases may then coexist on the surface, even at ambient.

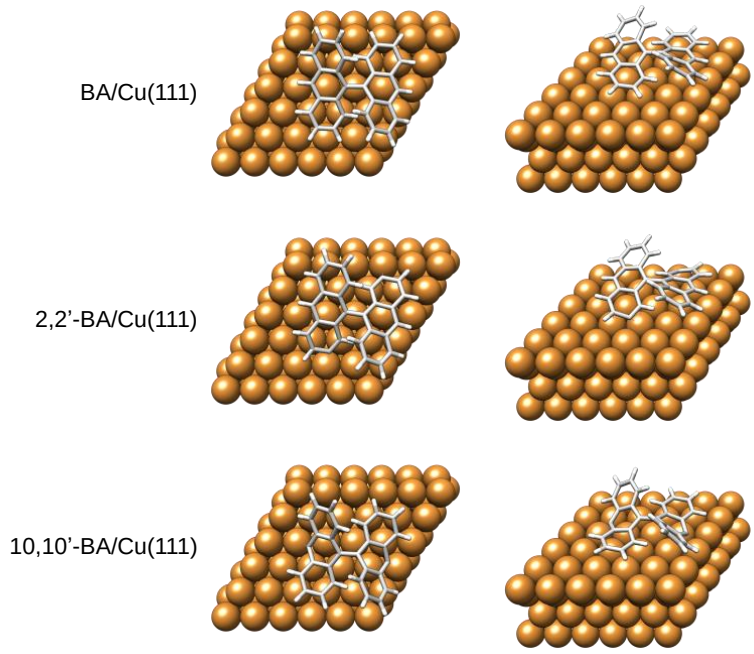

Fig. S8: DFT Simulation of BA molecule and its radical derivatives adsorbed onto a Cu(111) surface. The 2,2'-biradical is the more stable.

[1] P. Natarajan, M. Schmittel, *J. Org. Chem.* 203, **78**, 10383.
[2] N. Miyaura, A. Suzuki, *Chem. Rev.* 1995, **95**, 2457.
[3] J.M. Soler, E. Artacho, J.D. Gale, A. Garcia, J. Junquera, P. Ordejon, D. Sanchez- Portal, *J. Phys.: Condens. Matter* 2002, **14**, 2745.
[4] E.F. Pettersen, T.D. Goddard, C.C. Huang, G.S. Couch, D.M. Greenblatt, E.C. Meng, T.E. Ferrin, *J. Comput. Chem.* 2004, **25**, 1605.